A NUMERICAL ANALYSIS OF RECEIVING CHARACTERISTICS OF A H-PLANE TWO DIMENSIONAL HORN ANTENNA

Mampei NISHIMURA* and Hiroshi SHIGESAWA**
* Maizuru Technical College, Maizuru, 625 Japan
** Department of Electronics, Doshisha University, kyoto, 602 Japan

Introduction

A small sized horn antenna has often been used for primary radiator of aperture antennas. On finding efficiently numerical solutions of scattering problems, the authors have presented the Discrete Singularity Method(DSM) based on a nonlinear optimization technique[1]. This method is applied to find the directivity pattern as a receiving antenna, the fields scattered from it, and the receiving power when a small sized horn antenna is illuminated by a plane wave or a Gauss beam wave.

Numerical solutions and procedure

Fig.1 shows the physical configuration of the structure considered here, which consists of the two dimensional horn antenna and parallel plate waveguide. It is assumed that the incident wave $E_z^i(p)$ uniform in the z direction is an E-polarized wave traveling to the positive x direction, with exp(iωt) time dependence. The scattering field is also uniform in the z direction, and the problem to be considered becomes a two dimensional Dirichlet problem on the doundary. Our approach expresses the arbitrary field by using a set of fundamental solution $H_0^{(2)}(kr_t)$ (t=1,2,···,T) of two dimensional Helmholtz equation. Those singular points of the second order Hankel functions are arranged on a contour Γ inside the structure of which surface is expressed by the contour Γ'. Introducing now the unknown expansion coefficents A_t(t=1,2, ···,T), we approximate the scattering field by a truncated series as follows.

$$E_z^s(p)=\sum_{t=1}^{T} A_t H_0^{(2)}(kr_t), \tag{1}$$

where k is the wave number of free space and r_t is the distance from the t-th singularity to the observation point.

On the other hand, the incident wave E_z^i excites a field inside the waveguide. This field, if observed inside the waveguide around the origin, should be expressed in terms of a number of higher modes. However we assume that the waveguide can propagate only the dominant mode, so that the field $E_z^g(y)$ observed on a y-z plane at $x=l$ may be approximated by the dominant mode only. Assuming here that the waveguide is terminated with a matching load, E_z^g can be expressed as follows.

$$E_z^g(y)=A_0\cos(\pi y/a)\exp(j\beta(l-x)), \quad y\in S', \tag{2}$$

where β is the propagation constant of the dominat mode, a is the width of the parallel waveguide, A_0 is an unknown amplitude to be solved, and s' means the boundary region at $x=l$. To obtain $A_0, A, \cdots, A_T$, we apply the mode matching method based on the least-squares criterion in which the total field $E_z^i + E_z^s$ must be zero on the conductor and be continuous with E_z^g on s'. Then we can obtain the matrix equation for solving unknown coefficient A_0-A_T. To solve the above problem efficiently and accurately, it is quite important how to define the distribution of the singularity points. Therefore, our approach solves the positions of the singularities as well as the coefficients A_0 in the optimization process. This approach leads the problem to a nonlinear optimization problem.

Numerical results and Discussion

Let us define θ_i as the incidence angle of the input wave as shown in Fig.1. If θ_i are less than $\pi/2$, we may consider that the field scattered at the point B far from the aperture has negligible effect on the receiving field, and therefore the integration of the root mean-square errors on the conducting surface can be calculated along the finite boundary of Γ. The integration on the boundary s' is performed by putting $x=0.5\lambda$. For the nonlinear optimization the Gauss-Marquardt method is employed in this paper [2], and the initial positions of the singularities are arrayed on the Γ' with intervals of $\lambda/10$. Errors remain less than 0.5% after 10-th iterations.

Fig.2 shows the effective area(A_e) as a function of aperture angle (θ) for various flare length(L) in case of plane wave incident from $\theta_i=0$. In case of Gauss beam wave , the ratio P/W(P :receiving power, W : total input power) is shown as a function of θ for the various L for $w_0=1\lambda$ (w_0 :half-width of the Gauss beam wave). If A_e or P/W is calculated by changing the input angle θ_i for an antenna with specific values of L and θ, one can obtain the directivity pattern of an antenna. Fig.4 and 5 show such patterns for the plane wave or the Gauss beam wave incidence. We have an interest to understand the field behavior in the diffraction region. The coefficients $A_t (t=1,2, \cdots, T)$ have already been calculated, so that it is easy to calculate the total field at any point by using Eq.1. Fig.6 shows the calculated total field along the x axis for y=0. It is found that the standing wave with VSWR=1.22 exists even in the region less than $x=-6\lambda$.

Numerical results have shown that there is the optimum set of the flare angle and length of a small sized antenna for the E-polarized wave incidence. The further problems will be to find the receiving characteristics for the H-polarized incidence wave. More importantly, it is necessary to discuss the receiving characteristics of an antenna system with secondary reflector in junction with the field behavior around the reflector and the primary antenna.

Acknowledgment

The authors wish to thank Dr. K. Takiyama of the Doshisha University for encouragment during this work.

References

[1] M.Nishimura and H.Shigesawa, Trans. IECE of Japan, Vol. J66-B, No.2, pp245-252, Feb.1983.
[2] M.Nishimura, S.Takamatsu and H.Shigesawa, Trans. IECE of Japan, Vol.J67-B,No.5, pp552-558, May 1984.

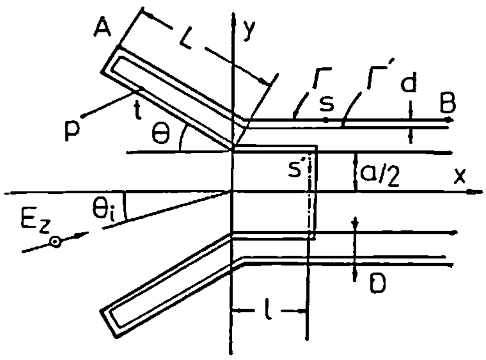

Fig.1. Two dimensional horn antenna and parallel plate waveguide.

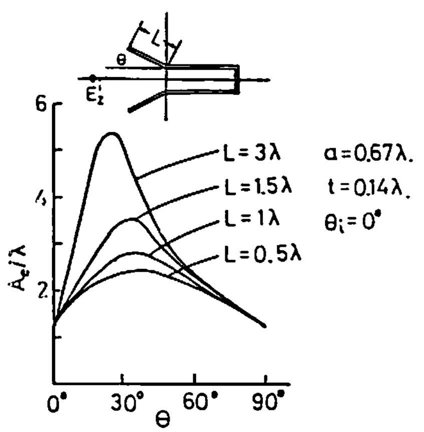

Fig.2. The effective area as a function of aperture angle for plane wave incidence.

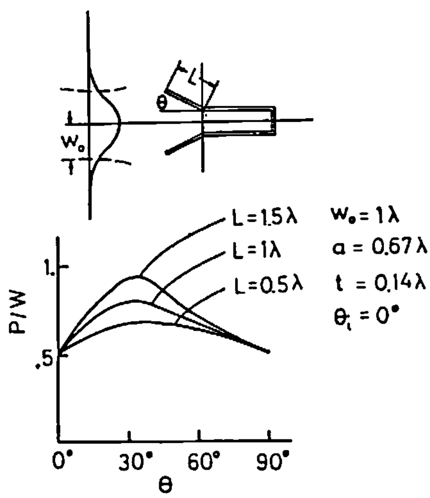

Fig.3. The ratio P/W as a function of aperture angle for Gauss beam wave incidence.

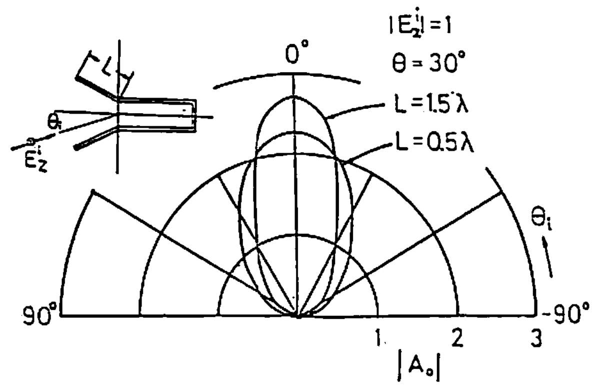

Fig.4. The directivity patterns for the plane wave incidence.

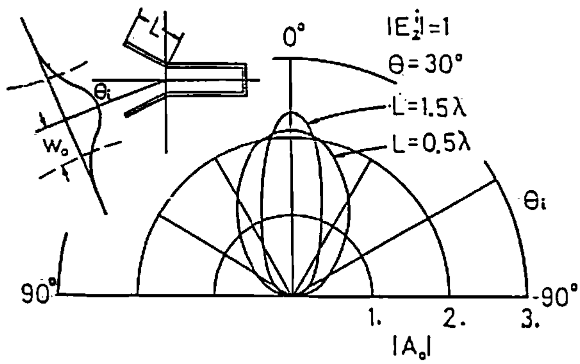

Fig.5. The directivity patterns for the Gauss beam wave incidence.

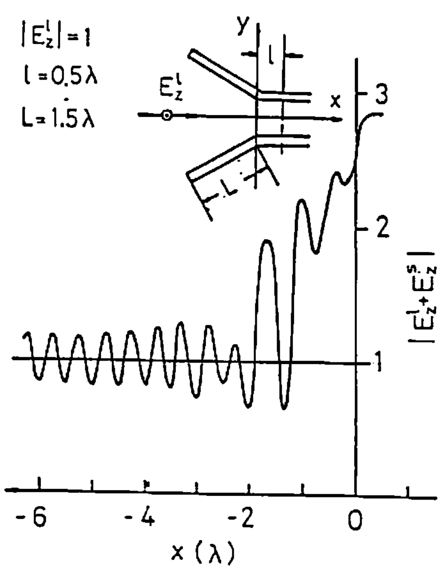

Fig. 6. The total field along the x axis.